Cortex Is Driven by Weak but Synchronously Active Thalamocortical Synapses

Randy M. Bruno* and Bert Sakmann

Sensory stimuli reach the brain via the thalamocortical projection, a group of axons thought to be among the most powerful in the neocortex. Surprisingly, these axons account for only ~15% of synapses onto cortical neurons. The thalamocortical pathway might thus achieve its effectiveness via high-efficacy thalamocortical synapses or via amplification within cortical layer 4. In rat somatosensory cortex, we measured in vivo the excitatory postsynaptic potential evoked by a single synaptic connection and found that thalamocortical synapses have low efficacy. Convergent inputs, however, are both numerous and synchronous, and intracortical amplification is not required. Our results suggest a mechanism of cortical activation by which thalamic input alone can drive cortex.

The thalamocortical (TC) projection has been intensely studied because the thalamus is part of the primary pathway by which information from the outside world is transmitted to the neocortex. Primary sensory nuclei of the thalamus contain cells whose axons project to the cortex, where they synapse mainly on dendrites of neurons in layer 4 (L4). L4 neurons respond to stimulation of the sensory periphery with large postsynaptic potentials (*1*–*3*). As these responses are initiated by direct monosynaptic inputs from the thalamus, TC axons have consequently been thought to comprise one of the most powerful "projection" systems in the brain (*4*, *5*). Paradoxically, thalamocortical synapses account for less than 15% of all synapses onto L4 spiny neurons (*6*).

The relative sparseness of thalamocortical synapses initially led to the assumption that the direct excitation provided by the thalamus is weak and requires amplification to activate the cortex (*5*, *7*, *8*). According to the "amplifier model," recurrent excitatory intracortical connections within L4 provide positive feedback during sensory stimuli and enhance the responses of cortical neurons. Computational models have demonstrated the feasibility of this hypothesis (*7*, *9*). It remains to be shown, however, that TC synapses actually require amplification simply because corticocortical synapses outnumber them.

High-efficacy TC synapses could alternatively ensure the strength of the TC projection. In vitro recordings from cortical neurons in acute (fresh) brain slices combined with minimal electrical stimulation of TC fiber tracts suggest that individual thalamocortical synapses are stronger and more reliable than corticocortical connections (*4*, *5*). Dual recordings could be used to explore this "strong-synapse model." Recording TC pairs, however, has not been feasible in vitro, because long-range connections are usually truncated during preparation of a cortical slice. Furthermore, the nature of the slice preparation prohibits the simultaneous study of functional properties, such as sensory-evoked responses.

These limitations could be overcome by dual recordings in the intact brain. Monosynaptic connections between cells in anesthetized animals have been putatively identified by recording extracellular action potentials (APs) and assessing the statistical probability with which "presynaptic" APs influence "postsynaptic" ones (*10*–*14*). Correlation analysis has additionally suggested an alternative "synchrony model," in which closely timed TC inputs are summed to strongly excite cortical cells directly (*15*). Extracellular AP recordings are limited, however, to inferring the presence of connections and cannot directly measure unitary excitatory postsynaptic potentials (EPSPs). Also, recorded cells are usually not identified in such experiments.

We present a new technique for measuring individual synaptic connections in vivo that overcomes such limitations. APs emitted by presynaptic thalamic cells are recorded extracellularly, while PSPs in postsynaptic cortical cells are simultaneously recorded intracellularly. The average EPSP is then determined by estimating and subtracting the contribution of unrecorded inputs.

Identification of monosynaptic connections in vivo. The TC projection in many sensory systems and species is organized topographically (*16*). The rodent whisker-barrel system is suited to studies where topographic alignment is critical. Rats have a stereotypical pattern of large facial whiskers, each of which drives neural activity in topographically aligned brain regions (*17*). The thalamic ventral-posterior medial (VPM) nucleus is subdivided into "barreloids" representing individual whiskers. L4 neurons in somatosensory cortex are similarly clustered into "barrels," which receive input predominantly from the corresponding barreloid (*16*, *18*, *19*).

Membrane potential (V_m) was recorded from a cortical neuron in an anesthetized or sedated rat [see Supporting Online Material (SOM)], while APs of a topographically aligned thalamic neuron were simultaneously recorded extracellularly (Fig. 1A). A synaptic connection between two neurons in vitro produces a small fluctuation (<4 mV) in postsynaptic V_m after each presynaptic AP (*5*, *20*, *21*). In vivo, however, barrages of thalamic and cortical postsynaptic potentials continuously generate much larger V_m fluctuations—up to 40 mV (Fig. 1A, upper trace; fig. S1). These obscure the EPSP evoked by any single thalamic AP (Fig. 1A, middle). This background "noise" can be overcome by averaging cortical V_m at the time of occurrence of each thalamic AP.

A simple average of V_m might be confounded by spontaneous APs discharged by near-synchronous thalamocortical neurons. In addition, collecting thousands of spontaneous APs to trigger an average would often exceed feasible recording times. Sensory stimuli have been thought to engage different degrees of synchrony among thalamic neurons (*22*, *23*), an idea that we exploited to evoke large numbers of APs while maintaining low levels of thalamic synchrony (see below and SOM). The synchrony of the afferent network was kept at a low level by deflecting the principal whisker (PW) with a small sinusoidal waveform (Fig. 1A, bottom trace). An AP- or "spike-triggered average" of cortical V_m was computed for periods of sinusoidal stimulation (Fig. 1B, top trace). The contribution of other inputs to V_m was estimated by shifting the records of V_m by one stimulus presentation and computing a new average V_m (Fig. 1B, middle trace). Subtraction of this new average from the first yields the average postsynaptic potential (aPSP) that a single thalamic AP evokes in the cortical cell (Fig. 1B, bottom trace; see Methods, SOM). An aPSP with short onset latency (2.4 ms) and typical rising and falling time courses of EPSPs at glutamatergic synapses (20 to 80% rise time 1.1 ms, decay 20 ms) is shown in Fig. 1C.

We also made a second test of connectivity in a subset of paired recordings. Hyperpolarizing current pulses were applied to the putative presynaptic thalamic neuron to evoke high-frequency AP bursts (Fig. 1E, lower traces), mediated by low-threshold voltage-dependent calcium channels. V_m of the cortical cell was then averaged with respect to the first AP in the burst (Fig. 1E, upper trace). The burst-triggered

Department of Cell Physiology, Max Planck Institute for Medical Research, Jahnstrasse 29, 69120 Heidelberg, Germany.

*To whom correspondence should be addressed. E-mail: bruno@mpimf-heidelberg.mpg.de

average (BTA) is several times larger than the aPSP (Fig. 1D), because each AP in the burst produces an aPSP that is summed with the others. Both tests of connectivity classified 10 out of 10 pairs equivalently (three out of three connected, seven out of seven unconnected).

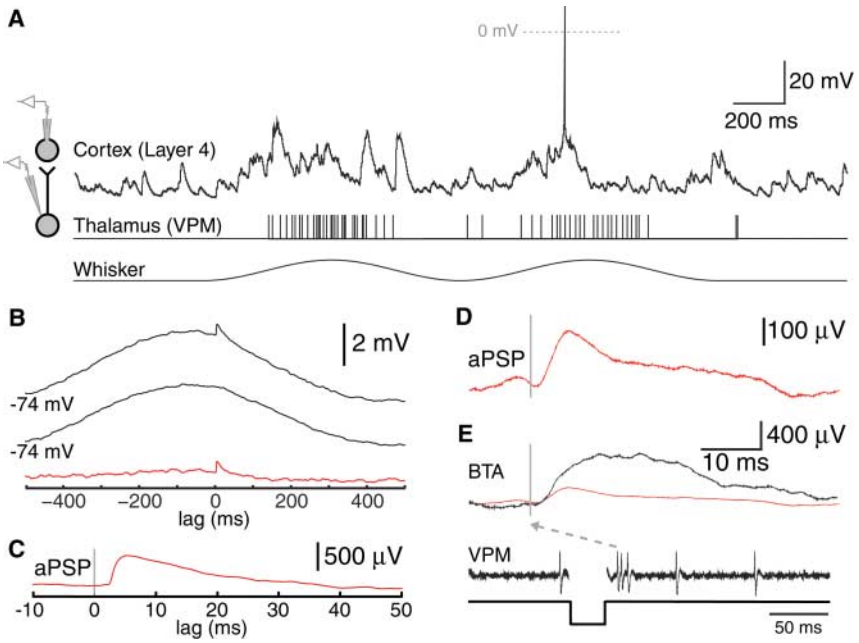

Fig. 1. Unitary connections are measurable in vivo. (**A**) Simultaneous intracellular recording of a cortical L4 neuron (Cortex) and extracellular recording of a somatotopically aligned thalamic neuron (Thalamus) during whisker stimulation (Whisker). (**B**) TC synapse onto an L4 spiny stellate. Top to bottom, Spike-triggered average, stimulus-induced correlation, difference giving aPSP (thalamic APs, $n = 1526$). (**C**) Expanded view of aPSP. (**D**) Example of one of the smallest aPSPs observed (thalamic APs, $n = 9900$). A star pyramid, 720 μm from the pia. (**E**) Electrical tests (black; n bursts = 460) for the same pair that produced the aPSP (red) in (D).

Probability and strength of TC connections. Thalamic neurons established direct monosynaptic connections onto L4 excitatory cells of all known morphologic types (Fig. 2). Spiny stellates have dendritic arbors that are confined to a barrel and lack an apical process (Fig. 2A). Spiny stellates are distinct from star pyramid cells, which have short apical dendrites that extend into layer 2/3 but do not reach layer 1 (Fig. 2B). Barrel star pyramids and spiny stellates received TC inputs with equal probability (10 out of 24 and 7 out of 11, respectively; five additional barrel neurons were spiny but not unambiguously star or stellate). No difference in aPSP amplitudes was observed between the two cell classes ($n = 9$ and $n = 7$, respectively, one connection BTA only, $P = 0.48$).

Monosynaptic connections onto excitatory L4 barrel neurons were frequently observed (17 out of 40 pairs, Fig. 3A). Onset latency, 20 to 80% rise time, and decay times were 1.72 ± 0.73, 3.38 ± 1.79, and 22.5 ± 24.7 ms (mean ± SD), respectively. The connections had small aPSP amplitudes (pooled over all animals: mean 950 μV ± 1.1 SD, median 550 μV, range 165 μV to 4.16 mV). TC-L4 synapses have previously been estimated on the basis of minimal stimulation in vitro to evoke larger EPSPs [mean 1.96 mV, range 0.39 to 5.89 mV (*5*)]. On the assumption that the number of release sites per connection and the efficacy of individual quanta of transmitter cannot be smaller in vivo, our data suggest that the TC

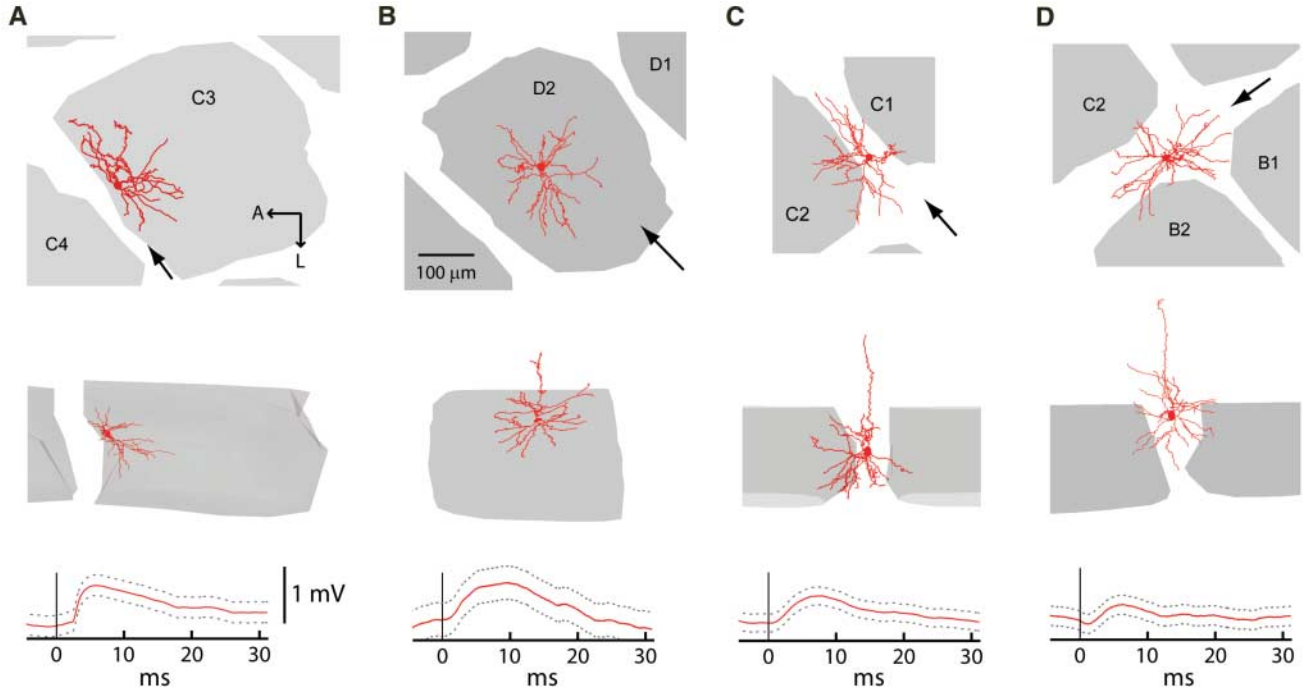

Fig. 2. TC synapses are made directly onto all types of excitatory L4 neurons. Upper row, tangential projections of 3-D reconstructions of four examples of connected cortical cells. Middle row, radial projection. Lower row, corresponding aPSP evoked by a paired thalamic neuron. Large arrows, approximate viewing angle for radial projection. *A*, anterior; *L*, lateral. Dashed lines, pointwise 99% confidence intervals. (**A**) Spiny stellate. (**B**) Star pyramid. (**C**) Interrow septum neuron. (**D**) Interarc septum neuron.

synapse in vivo may have a probability of release much lower than observed in vitro (*4*).

One possible explanation for a drop in release probability is that, in acute brain slices, thalamic axons are almost completely inactive. TC neurons have, however, substantial spontaneous AP rates in both the anesthetized and sedated rats used here (medians 1.0 and 5.4 Hz, respectively) as in the awake rat (*24*). Such high firing rates are likely to cause TC synapses to be continuously depressed in vivo (*25*, *26*). Consistent with this hypothesis, aPSPs of TC-barrel neuron connections were smaller during sedation (median 0.24, range 0.17 to 1.57, mean 0.49 ± 0.13 mV, $n = 11$; $P = 0.028$) than during anesthesia (median 1.3, range 0.25 to 4.16, mean 1.94 ± 0.67 mV, $n = 5$). Depression is also observable when estimating aPSPs from APs divided into subsets by the preceding interspike interval (Fig. 3C). Thus, as thalamic activity increases, TC efficacy decreases. The dependency of aPSP size on ongoing presynaptic AP rate likely explains why strong adaptation of sensory responses seen under anesthesia (*27*) are almost absent in the awake rat (*28*). Thus, individual thalamocortical synapses in the awake animal may be no more effective than typical corticocortical synapses.

Pairs of thalamic and topographically unaligned L4 cells were unconnected, as were pairs involving layer 2/3 cells (Fig. 3A), consistent with the known sparse lemniscal pathway projection to these regions (*18*). We also investigated pairs in which cortical cells were located in the neighboring "septum," interbarrel regions innervated by relatively few VPM axons and thought to be part of the paralemniscal system (*18*, *29*). Surprisingly, septum cells are as likely as barrel neurons to receive input from VPM, which belongs to the lemniscal system (6 out of 14 pairs; Fig. 3A). During sedation, strengths of TC connections onto septum neurons (Fig. 3B; mean 0.40 ± 0.05 mV, $n = 4$) did not differ from those onto barrel neurons (0.49 ± 0.13 mV, $n = 11$, $P = 0.85$), although their similarity may have been due to the small sample size. Monosynaptic connections were observed for septum neurons between both arcs (Fig. 2C) and rows (Fig. 2D). Our observations are consistent with the known morphology of septum neurons (*30*), which extend dendrites into barrels (Fig. 2, C and D). These data suggest that the septum, like other regions (*20*), integrates lemniscal and paralemniscal pathways.

Cortical neurons are known to fluctuate between depolarized ("up") and hyperpolarized ("down") states (*1*, *31*). In the anesthetized animal, we observed typical up and down states in cortical neurons. Such obvious bistability is not seen in L4 neurons in the sedated animal (Fig. 1A) or in the awake animal (fig. S5A). Nevertheless, cortical V_m still fluctuates between depolarized and hyperpolarized levels (Fig. 1A). Thus, the efficacy of single TC synapses may depend on the variable conductance state of the recipient neuron. This possibility was examined by computing aPSPs separately for thalamic APs occurring when a barrel neuron was already "depolarized" or "hyperpolarized," defined here as having a V_m greater or less, respectively, than the median. Figure 3D1 shows an example in which aPSP amplitude during hyperpolarized V_m is three times that seen in a depolarized V_m. An aPSP for a given connection tended, on average, to be larger during hyperpolarized V_m (Fig. 3E, mean increase 0.34 ± 0.19 mV, $n = 22$, $P = 0.03$), but some connections exhibited no difference between states or even the reverse. A similar analysis using electrically evoked thalamic bursts was therefore made for the pair shown in Fig. 3D2. BTAs for this connection were similar during hyperpolarization and depolarization (Fig. 3D2), which indicates that observations lacking a difference between states are not simply due to noise in aPSP estimation. These exceptions may be due to one or more of the following: (i) V_m differences between the soma and the distal dendrites where TC synapses are located, (ii) anomalously rectifying voltage-gated channels, or (iii) dendritic shunting (*32*).

Synchronous subnetworks. What do individual TC connections contribute to the subthreshold activity of cortical cells? Numerous thalamocortical and intracortical axons contact any given L4 neuron and generate compound excitatory and inhibitory PSPs. Combined, they produce spontaneous and stimulus-evoked changes in cortical V_m (Fig. 1A). For example, Fig. 4C shows average net PSPs evoked in a L4 spiny stellate by deflection of its PW in each of eight directions (gray zones). The largest net excitatory PSPs to deflection onset were observed for only a limited range of stimulus directions. Deflections in opposite directions evoked the largest stimulus-offset PSPs (e.g., 45° to 135°). Sustained depolarization is also seen between onset and offset for 180° and 225°. This cortical cell received a monosynaptic connection from the thalamic neuron whose stimulus-evoked APs are shown as peristimulus time histograms (PSTHs) (Fig. 4A).

The excitation that this individual thalamic neuron contributes to the cortical cell's responses can be estimated by convolving the PSTHs of thalamic APs with the aPSP of the single connection (Fig. 4B). Despite the thalamic cell's substantial spontaneous and evoked activity, its total excitatory contribution to the cortical cell is, at all times, less than 1 mV. Possible synaptic dynamics, which could only further decrease this value, were not modeled.

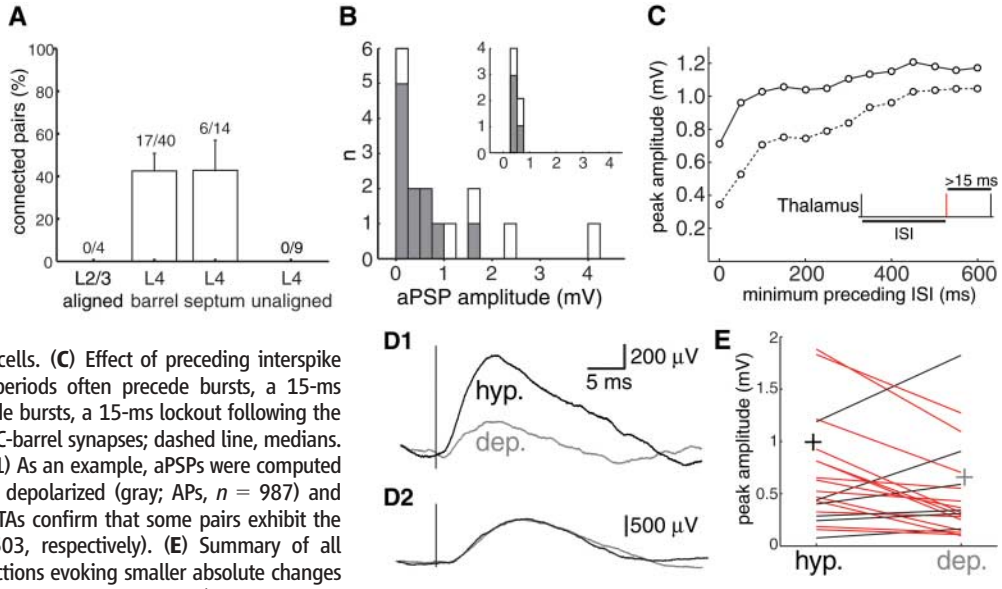

Fig. 3. TC synapses are numerous but weak. (**A**) Proportion of connected pairs involving thalamic cells and spiny cortical cells in various locations (aligned layer 2/3, aligned barrels, septum neighboring aligned barrels, and unaligned L4). Standard error bars calculated for a binomial distribution. (**B**) Amplitude distribution for pairs involving spiny barrel neurons. One connection was studied only by BTAs and, therefore, had no measurable aPSP. The histogram is divided into subsets according to preparation: filled, sedation; white, anesthesia. Inset, Same for septum cells. (**C**) Effect of preceding interspike interval (ISI) on amplitude. Because quiet periods often precede bursts, a 15-ms successor interval was also imposed. To exclude bursts, a 15-ms lockout following the AP was applied (inset). Solid line, means for TC-barrel synapses; dashed line, medians. (**D**) aPSPs are modulated by cortical state. (D1) As an example, aPSPs were computed for APs occurring when the cortical cell was depolarized (gray; APs, $n = 987$) and hyperpolarized (black; APs, $n = 821$). (D2) BTAs confirm that some pairs exhibit the reverse or no effect (APs, $n = 483$ and 503, respectively). (**E**) Summary of all connections, analyzed as in (D1). Red, connections evoking smaller absolute changes during depolarization. For visualization, two red pairs are not shown (hyperpolarized-depolarized values: 6.15 and 2.1 for one, 2.25 and 2.20 for the other, respectively). Plus signs (+) are means (hyperpolarized, 0.99; depolarized, 0.66).

Thus, even for stimulus-evoked AP trains, cortical excitation produced by any individual connection is relatively small. Nevertheless, the overall time course and directional tuning of the single thalamic input (Fig. 4B) and net cortical excitation produced by multiple inputs (Fig. 4C) are remarkably similar. Not all inputs to the cortical neuron are identical: The single TC input contributes nothing to the robust cortical onset response at 315°, which is evoked by other inputs.

We compared the tuning curves of the thalamic and cortical cell populations. Polar plots of the total AP response to each direction of whisker movement were constructed for every thalamic neuron, aligned to their preferred angles, and averaged (Fig. 4D). Thalamic neurons exhibited substantial directional tuning, and the average polar plot of PSPs in cortical cells mirrors this degree of tuning (compare Fig. 4D with Fig. 4F, red). Tuning at the level of APs is sharpened by the spike threshold (Fig. 4F, blue, and fig. S4) as previously found (*33*). No overall directional bias was observed for the cortical neuron population (Fig. 4E; $P = 0.73$ for caudorostral axis; $P = 0.45$ ventrodorsal; $n = 44$ cells). Thus the strong correspondence between thalamic AP output and cortical EPSP input cannot be due to a directional bias in the trigeminal pathway. Rather, their correspondence suggests that a select and potentially synchronous subpopulation of thalamic neurons converges on any given excitatory L4 cell. If this were not the case, the directional tuning of the L4 population would be significantly broader.

Therefore, we quantified the similarity of directional tuning of pairs by calculating correlation coefficients for corresponding thalamic and cortical polar plots. Examples with varying degrees of similarity are shown in Fig. 5A to C. Pairs of connected cells were similarly tuned (Fig. 5D; mean 0.37 ± 0.13, $P = 0.01$). Pairs without connection were both of similar or dissimilar tuning (Fig. 5E; mean –0.07 ± 0.17, $P = 0.7$). Consistent with extracellular findings in the somatosensory (*11*), auditory (*14*), and visual systems (*12*), converging TC inputs onto excitatory neurons are similarly tuned, likely thereby endowing the target cortical neuron with similar tuning.

Previous studies of VPM, using averages of local field potentials (*23*) and population PSTHs of sequentially recorded single units (*22*), suggested that relatively high-velocity whisker stimuli, such as those used here, on average evoke strong synchrony among thalamic inputs. To directly assess near-synchronous discharge of thalamic inputs on a trial-by-trial basis, we made simultaneous extracellular recordings of multiple VPM neurons (Fig. 6, A and B), either on one electrode or two different electrodes in the same barreloid. To be included in analyses, cells recorded on the same electrode were required to have nonoverlapping AP waveform distributions (see SOM). For each pair, cross-correlation histograms were made separately for spontaneous and stimulation periods (Fig. 6, C and D), and the number of near-synchronous events on the time scale of an EPSP was quantified by using a simple measure that normalizes for the firing rates of the two neurons (see SOM).

Weak synchrony is sometimes observed during spontaneous activity (Fig. 6C and fig. S6). For the same thalamic pair, high-velocity whisker stimulation noticeably enhances thalamic synchrony (Fig. 6D). Across the 28 pairs recorded, thalamic synchrony was typically

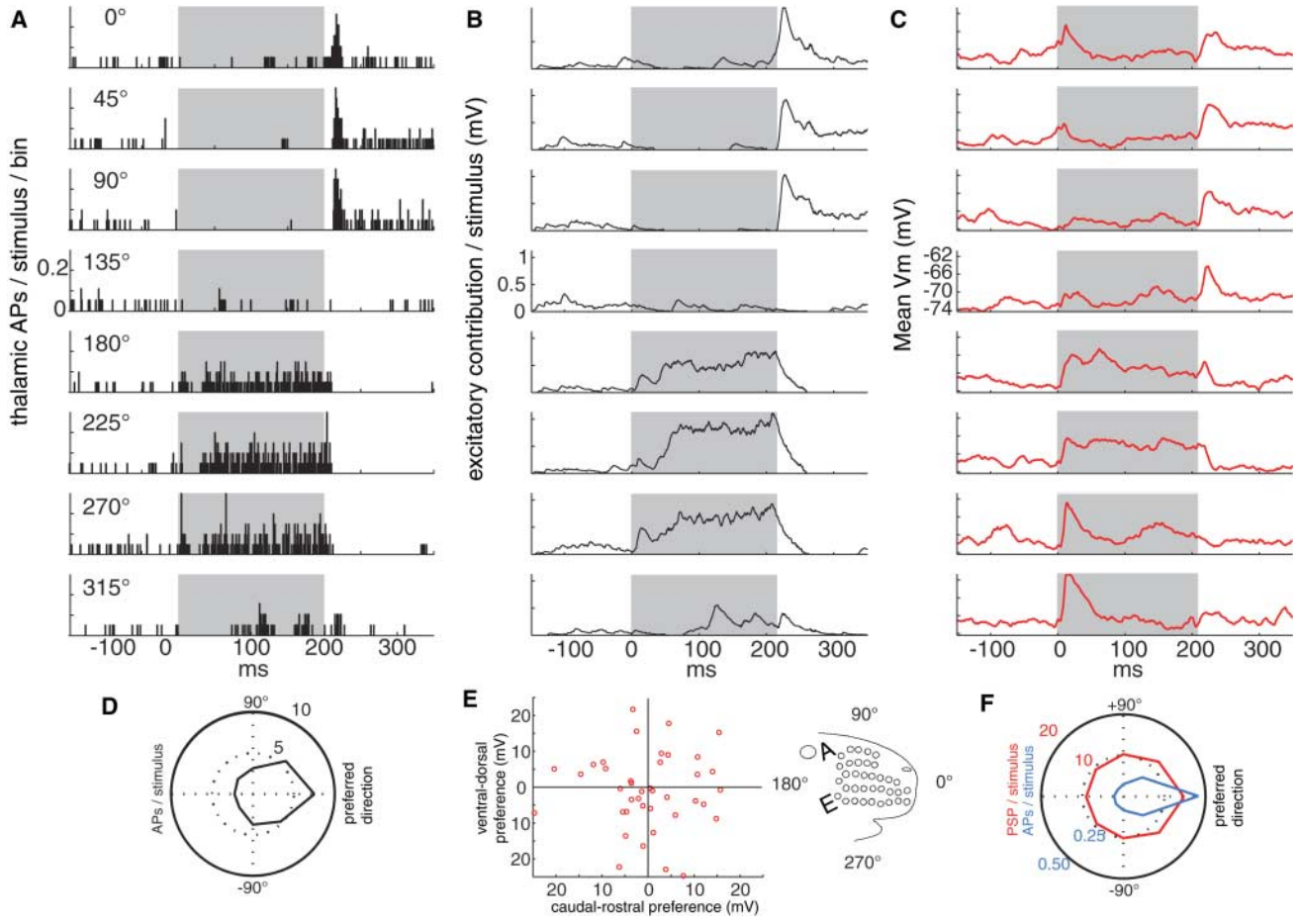

Fig. 4. Net synaptic inputs to a cortical cell closely resemble a single thalamic input. (**A**) PSTHs of APs of a thalamic neuron in response to 20 whisker deflections (gray) in each of 8 directions. (**B**) Excitation provided by the neuron in A. (**C**) PSP responses of a cortical cell postsynaptic to this thalamic cell. (**D**) Average tuning curve for thalamic cell population ($n = 21$) during 200 ms following stimulus onset. (**E**) Scatter plot of cortical cell directional preferences. Layout of rat facial whiskers (rows A to E) with regard to polar plots. (**F**) Same as (D) but for cortical cells ($n = 40$). Red, PSPs; blue, APs.

increased by the high-velocity stimulus (Fig. 6E; paired t test, $P < 10^{-4}$). In contrast, the low-velocity sinusoid used to evoke thalamic APs during aPSP estimation did not increase synchrony (fig. S6C; $P = 0.28$, $n = 19$). Results were equivalent for subsets of the data containing only pairs recorded on the same or different electrodes (see SOM). In conclusion, at the level of individual presentations, sensory stimulation can induce synchronous discharge of thalamic neurons.

Architecture of the thalamocortical pathway. The typical aPSP measures 490 μV whereas the average subthreshold response of a barrel neuron to a preferred stimulus is ~15 mV. Interestingly, field potentials averaged with regard to spontaneous thalamic discharges and sensory stimuli exhibit a similar ratio (*34*). If one considers only TC–spiny barrel neuron connections, then a minimum of 30 thalamic cells could account for stimulus-evoked cortical responses. However, because of additional contributions of feed-forward inhibition (*11*, *13*, *35*) and feedback excitation/inhibition (*3*, *21*, *36*), 30 thalamic inputs is likely an underestimate. Our method suggests a TC convergence ratio of ~0.43, consistent with paired extracellular estimates (*11*), but slightly higher, perhaps because of better sensitivity to weak connections. Therefore, given ~200 thalamic cells per barreloid (*16*, *37*), a L4 cell would on average receive ~85 TC connections (200 cells × 0.43 connections/cell).

About 65% of the roughly 2800 total spines on dendrites of an excitatory L4 neuron are contacted by axons originating from other L4 cells (*8*), which leaves slightly fewer than 1000 spines available for other inputs, such as TC axons. Each TC axon is thought to contribute on average about seven active synaptic contacts (*4*). Our estimate of 85 TC connections per cell suggests that, on average, 600 spines would be contacted by TC axons. This is well within the range of the 1000 spines not associated with axons originating within L4.

Our approach demonstrates that cross-correlation analysis of extracellular data, a technique introduced 40 years ago (*10*) and since used in a variety of systems, can correctly infer monosynaptic connections. Interestingly, paired extracellular recordings find correlogram peaks having latencies of ~2 ms—the same as that of EPSPs here and in vitro (*4*, *5*). This suggests that cortical APs are triggered on the EPSP rising phase rather than at the peak, consistent with reports that neurons are sensitive to the rate of V_m change, as well as absolute V_m (*33*, *38*). Overall time course of aPSPs is slower than that of EPSPs in vitro, perhaps because of jitter during averaging, weaker driving force in vivo, and/or larger contributions of *N*-methyl-D-aspartate receptors in vivo.

Individual TC synapses in vivo appear to be weaker than previously thought from slice studies. This difference may reflect inadvertent activation of multiple axons during "minimal stimulation" in vitro. A more likely explanation is that driving force is reduced in vivo, lessening the impact of any individual TC synapse. Additionally, the relatively high firing rates of thalamic neurons persistently depress TC synapses in vivo, as previously indicated by electrical thalamic stimulation (*25*, *26*). Our measurements demonstrate such depression at the level of unitary EPSPs. Cortical neurons in vivo, however, have lower spontaneous and evoked firing rates than thalamic neurons (*1*, *11*, *17*, *39*), and corticocortical synapses may consequently be less depressed than TC synapses. If this is the case, they may have strengths similar to those observed here. Somatosensory corticocortical connections have not yet been measured in vivo. One study in monkey motor cortex (*40*) observed similar unitary corticocortical connections (mean 226 μV), but a unitary EPSP

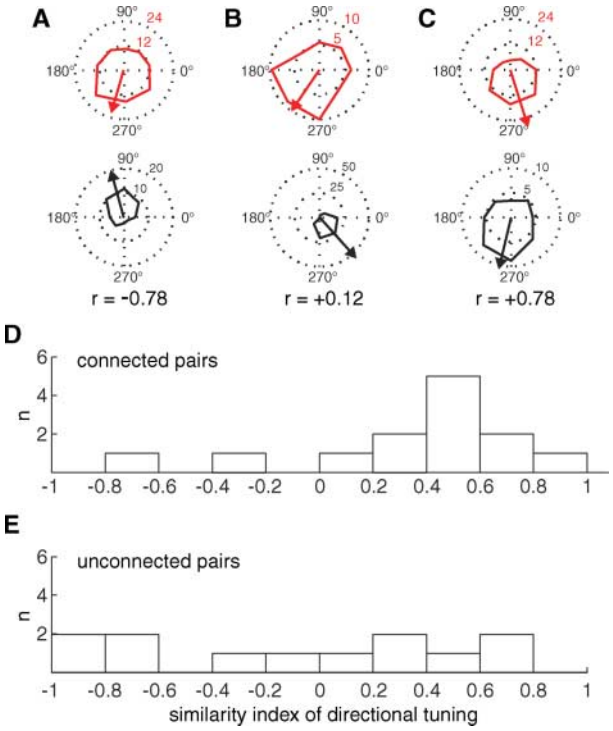

Fig. 5. Converging TC inputs have similar directional tuning. (**A** to **C**) Polar plots of example connected pairs having varying degrees of directional tuning similarity. Red, mean cortical PSP amplitudes (mV); black, mean thalamic spikes per stimulus. *r*, correlation of the polar plots. (**D**) Distribution of directional tuning similarity for connected pairs. (**E**) Distribution for unconnected pairs.

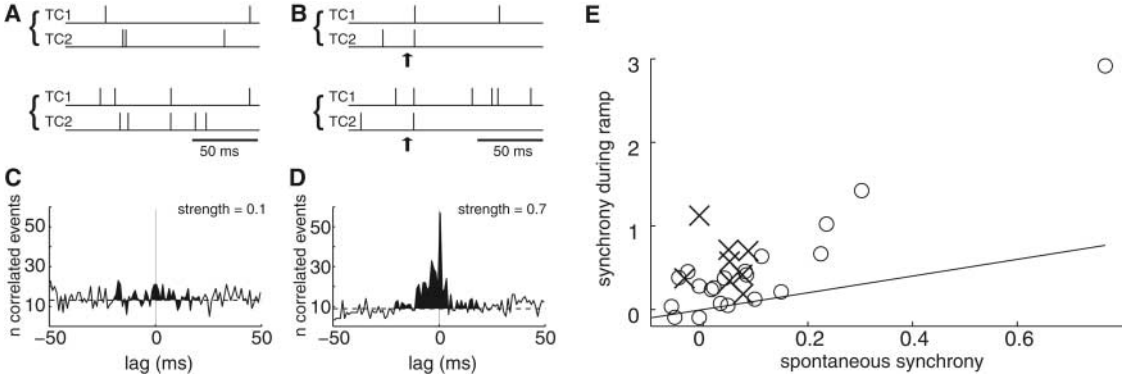

Fig. 6. High-velocity stimuli synchronize TC neurons. (**A**) Spontaneous APs from two TC neurons (*TC1*, *TC2*) recorded simultaneously on two electrodes in the same barreloid during sedation. Braces, simultaneously recorded APs. (**B**) Same pair during whisker stimuli (arrows). (**C** and **D**) Cross-correlation histograms of pair during spontaneous (C) and sensory-evoked (D) activity (trigger events, n = 419 and 395, respectively; 1-ms bins). Long dash, baseline; shading, events above baseline in ±20-ms window. (**E**) Synchrony during high-velocity stimuli is stronger than during spontaneous periods. Line, unity; circle, pair recorded on same electrode; X, pair recorded on two separate electrodes.

could not be determined for 90% of pairs, as it was not possible to estimate and subtract out other synaptic inputs as we did.

Layer 4 networks have been thought to amplify the output of a weak thalamocortical pathway (*5*, *7*, *8*). Although individual TC connections are indeed relatively weak and alone are unable to drive cortical activity, each cortical cell in L4 is the target of substantial numbers of converging TC synapses. Strong sensory stimulation elicits a near-synchronous pattern of APs among the majority of these converging inputs. Such an input pattern affords strong feed-forward excitation on the order of 10s of millivolts, which exceeds the size of the net sensory-evoked PSPs observed here and previously for L4 neurons (*1*–*3*). Recurrent excitatory connections in L4 are, therefore, not required to account for such large PSPs.

References and Notes

1. M. Brecht, B. Sakmann, *J. Physiol.* **543**, 49 (2002).
2. D. Ferster, S. Chung, H. Wheat, *Nature* **380**, 249 (1996).
3. M. Wehr, A. M. Zador, *Nature* **426**, 442 (2003).
4. Z. Gil, B. W. Connors, Y. Amitai, *Neuron* **23**, 385 (1999).
5. K. J. Stratford, K. Tarczy-Hornoch, K. A. Martin, N. J. Bannister, J. J. Jack, *Nature* **382**, 258 (1996).
6. G. Benshalom, E. L. White, *J. Comp. Neurol.* **253**, 303 (1986).
7. R. J. Douglas, C. Koch, M. Mahowald, K. A. Martin, H. H. Suarez, *Science* **269**, 981 (1995).
8. J. Lübke, V. Egger, B. Sakmann, D. Feldmeyer, *J. Neurosci.* **20**, 5300 (2000).
9. H. Suarez, C. Koch, R. Douglas, *J. Neurosci.* **15**, 6700 (1995).
10. D. H. Perkel, G. L. Gerstein, G. P. Moore, *Biophys. J.* **7**, 419 (1967).
11. R. M. Bruno, D. J. Simons, *J. Neurosci.* **22**, 10966 (2002).
12. R. C. Reid, J. M. Alonso, *Nature* **378**, 281 (1995).
13. H. A. Swadlow, A. G. Gusev, *Nat. Neurosci.* **5**, 403 (2002).
14. L. M. Miller, M. A. Escabi, H. L. Read, C. E. Schreiner, *Neuron* **32**, 151 (2001).
15. J. M. Alonso, W. M. Usrey, R. C. Reid, *Nature* **383**, 815 (1996).
16. P. W. Land, S. A. Buffer Jr., J. D. Yaskosky, *J. Comp. Neurol.* **355**, 573 (1995).
17. D. J. Simons, G. E. Carvell, *J. Neurophysiol.* **61**, 311 (1989).
18. S. M. Lu, R. C. Lin, *Somatosens. Mot. Res.* **10**, 1 (1993).
19. P. B. Arnold, C. X. Li, R. S. Waters, *Exp. Brain Res.* **136**, 152 (2001).
20. D. Feldmeyer, A. Roth, B. Sakmann, *J. Neurosci.* **25**, 3423 (2005).
21. D. Feldmeyer, V. Egger, J. Lübke, B. Sakmann, *J. Physiol.* **521**, 169 (1999).
22. D. J. Pinto, J. C. Brumberg, D. J. Simons, *J. Neurophysiol.* **83**, 1158 (2000).
23. S. Temereanca, D. J. Simons, *J. Neurophysiol.* **89**, 2137 (2003).
24. E. E. Fanselow, M. A. Nicolelis, *J. Neurosci.* **19**, 7603 (1999).
25. M. A. Castro-Alamancos, *Prog. Neurobiol.* **74**, 213 (2004).
26. C. E. Boudreau, D. Ferster, *J. Neurosci.* **25**, 7179 (2005).
27. S. Chung, X. Li, S. B. Nelson, *Neuron* **34**, 437 (2002).
28. M. A. Castro-Alamancos, *Neuron* **41**, 455 (2004).
29. E. Ahissar, R. Sosnik, S. Haidarliu, *Nature* **406**, 302 (2000).
30. D. J. Simons, T. A. Woolsey, *J. Comp. Neurol.* **230**, 119 (1984).
31. J. Anderson, I. Lampl, I. Reichova, M. Carandini, D. Ferster, *Nat. Neurosci.* **3**, 617 (2000).
32. J. Waters, F. Helmchen, *J. Neurosci.* **24**, 11127 (2004).
33. W. B. Wilent, D. Contreras, *J. Neurosci.* **25**, 2983 (2005).
34. H. A. Swadlow, A. G. Gusev, T. Bezdudnaya, *J. Neurosci.* **22**, 7766 (2002).
35. L. Gabernet, S. P. Jadhav, D. E. Feldman, M. Carandini, M. Scanziani, *Neuron* **48**, 315 (2005).
36. D. J. Pinto, J. A. Hartings, J. C. Brumberg, D. J. Simons, *Cereb. Cortex* **13**, 33 (2003).
37. C. Varga, A. Sik, P. Lavallee, M. Deschenes, *J. Neurosci.* **22**, 6186 (2002).
38. R. Azouz, C. M. Gray, *Proc. Natl. Acad. Sci. U.S.A.* **97**, 8110 (2000).
39. M. Brecht, B. Sakmann, *J. Physiol.* **538**, 495 (2002).
40. M. Matsumura, D. Chen, T. Sawaguchi, K. Kubota, E. E. Fetz, *J. Neurosci.* **16**, 7757 (1996).

41. Thanks to C. de Kock, D. Feldmeyer, D. Haydon-Wallace, M. Helmstaedter, P. Krieger, P. Medini, P. Osten, and H. Spors for comments on the manuscript; M. Kaiser, R. Roedell, K. Schmidt, and E. Stier for outstanding technical assistance; and B. Gaertner, V. Hotz, M. Maerz, R. Masionyte, S. Tokur, and S. Wiegert for morphological reconstructions. Support provided by the Max Planck Society.

Supporting Online Material

www.sciencemag.org/cgi/content/full/312/5780/1622/DC1
Materials and Methods
SOM Text
Figs. S1 to S7
References

4 January 2006; accepted 5 May 2006
10.1126/science.1124593

Biomarker Evidence for a Major Preservation Pathway of Sedimentary Organic Carbon

Y. Hebting,[1]* P. Schaeffer,[1] A. Behrens,[1] P. Adam,[1] G. Schmitt,[1] P. Schneckenburger,[1] S. M. Bernasconi,[2] P. Albrecht[1]†

Hydrogenation processes leading from biomolecules to fossil biomarkers in anoxic sediments are crucial for the preservation of organic matter. However, these processes are still poorly understood. The present identification of several reduced carotenoids in recent sediments attests that these processes operate at the earliest stages of diagenesis without structural or stereochemical specificity, implying a nonbiological reduction pathway. Sulfur species (e.g., H_2S) are the hydrogen donors involved in such reduction, as demonstrated with laboratory experiments. These reactions allow the preservation of abundant organic carbon in the rock record.

High sedimentation rates, sorption onto mineral surfaces, humification reactions, and intrinsic resistance to biodegradation of naturally occurring biopolymers are important factors associated with the preservation of organic carbon in sediments, depending upon the environment (*1*). In organic-rich marine sediments, which are usually associated with oxygen-depleted depositional environments and which eventually lead to major petroleum deposits by thermal evolution (*2*), enhanced preservation is attributed mainly to efficient reduction processes and sulfurization (*3*, *4*).

The reduction reactions, generally referred to incorrectly as "hydrogenation," have been invoked as being responsible for the defunctionalization of biological lipids, leading to biomarker hydrocarbons present in fossil organic matter. The most classical examples are the widespread occurrence in the geosphere of biomarker hydrocarbons such as β-carotane, phytane, steranes, and hopanes deriving, respectively, from β-carotene, phytol-related terpenoids, steroids, and hopanoids present in various organisms of mainly algal and bacterial origin. The role of late diagenetic or catagenetic thermal processes in the formation of sedimentary hydrocarbons through a sequence of cracking and hydrogen transfer reactions is well described (*5*), leading to petroleum, gases, and graphitized material. In contrast, only a few studies have been devoted to the effective reductive alteration of sedimentary organic carbon during early diagenesis, despite the major role that this process certainly plays in the transformation and preservation of organic material in the geosphere.

It has been proposed that biological processes intervene in the reductive transformation undergone by sedimentary organic carbon at the first stages of sedimentation, as is the case of the conversion of sterols to stanols (*6*, *7*). However, such transformations might also result from purely chemical, abiotic reactions, although this has not been clearly established, except for in some xenobiotics, which are reduced in natural environments (*8*).

We investigated this problem on a molecular basis by studying the reductive transformations undergone by carotenoids as precursors in recent sediments deposited in the lake of Cadagno (Switzerland), an ideally suited model system of sulfide-rich, anoxic environment (*9*, *10*). In addition, we developed laboratory experiments demonstrating that the sulfides formed by bacterial sulfate reduction are most likely to be the reducing agents responsible for the reduction affecting decaying carotenoids and other lipids in the water column and within the sediment.

[1]Laboratoire de Géochimie Bioorganique, Unité Mixte de Recherche 7509 du CNRS, Université Louis Pasteur, Ecole de Chimie, Polymères, Matériaux de Strasbourg, 25 rue Becquerel, 67200 Strasbourg, France. [2]Geologisches Institut, ETH Zürich, CH-8092 Zürich, Switzerland.

*Present address: Department of Earth, Atmospheric, and Planetary Sciences, Massachusetts Institute of Technology, 77 Massachusetts Avenue, Cambridge, MA 02139, USA.
†To whom correspondence should be addressed. E-mail: albrecht@chimie.u-strasbg.fr